NANO LETTERS

2009
Vol. 9, No. 5
1989-1993

Selective Excitation and Detection of Spin States in a Single Nanowire Quantum Dot

Maarten H. M. van Weert,[†] Nika Akopian,[†] Umberto Perinetti,[†] Maarten P. van Kouwen,[†] Rienk E. Algra,[‡,§] Marcel A. Verheijen,[‡] Erik P. A. M. Bakkers,[‡] Leo P. Kouwenhoven,[†] and Val Zwiller*[,†]

Kavli Institute of Nanoscience, Delft, The Netherlands, and Philips Research Laboratories, Eindhoven, The Netherlands

Received January 23, 2009; Revised Manuscript Received March 4, 2009

ABSTRACT

We report exciton spin memory in a single $InAs_{0.25}P_{0.75}$ quantum dot embedded in an InP nanowire. By synthesizing clean quantum dots with linewidths as narrow as about 30 μeV, we are able to resolve individual spin states at magnetic fields on the order of 1 T. We can prepare a given spin state by tuning excitation polarization or excitation energy. These experiments demonstrate the potential of this system to form a quantum interface between photons and electrons.

The unprecedented material and design freedom makes semiconducting nanowires very attractive for novel optoelectronics.[1−4] Quantum dots incorporated in nanowires enable experiments on both quantum optics [5−7] and electron transport.[8] This system has the potential to form a quantum interface between these separate fields of research. A crucial element for such interface is control over the spin of an exciton by means of photon polarization. Optical spectra of such nanowire quantum dots, however, have so far been hampered by broad linewidths, insufficient for identifying quantum states. Here, we demonstrate clean $InAs_{0.25}P_{0.75}$ quantum dots embedded in InP nanowires with excellent optical quality. Narrow linewidths enable us to selectively excite and detect single exciton spins. We control spin excitation by the polarization or the energy of the excitation light. The dots exhibit exciton-spin memory demonstrating that nanowires are a viable alternative to the system of self-assembled dots with new design options to interface single photon [9,10] with single electron devices.[11,12]

Photoluminescence (PL) from homogeneous nanowires [13,14] and from quantum dots (QDs) embedded in nanowires[15] is highly linearly polarized for light emitted perpendicular to this 1D geometry. This forms an important obstacle for controlling the spin states of excitons for which circularly polarized light is needed. Circular polarization requires the light to be precisely aligned along the nanowire axis, since nanowires are circularly symmetric around this axis. Here we report such a study on as-grown, vertical nanowires standing parallel to our optical axis. We demonstrate full optical access to the spin states of individual excitons by means of right and left circularly polarized photons.

Exciton spin states have been studied extensively in self-assembled quantum dots.[16] Quantum dots in nanowires are a promising alternative to self-assembled dots when it comes to more complex circuits. For instance, multiple dots are naturally aligned in nanowires;[17] heterostructure dots can be connected to gate-defined dots;[18] and circuits of dots can be integrated with pn-junctions to allow for electroluminescence and photocurrent experiments. Also local gating of heterostructure dots in nanowires has become possible with recently developed wrap-around gates.[19−21] These promises motivate the development of clean nanowire quantum dots where cleanliness is measured as a narrow line width in the optical spectra. Initial optical studies of nanowire quantum dots reported linewidths on the order of millielectronvolts,[5−7] which is a thousand times broader than expected for the natural line width (i.e., the inverse radiative lifetime of about 1 ns). Such broad lines hampered resolving individual spin states. Here, we report on clean nanowire quantum dots with optical linewidths of tens of millielectronvolts, i.e., sufficiently sharp for measuring spin states above a magnetic field of ∼1 T.

We grow $InAs_{0.25}P_{0.75}$ quantum dots embedded in InP nanowires (see methods and refs 17, 22, and 23). Figure 1a shows an image of our sample with bright spots from the

* E-mail address: v.zwiller@tudelft.nl.
[†] Kavli Institute of Nanoscience.
[‡] Philips Research Laboratories.
[§] Also at Materials Innovation Institute (M2I), Delft 2628CD, The Netherlands, and IMM, Solid State Chemistry, Radboud University Nijmegen, Nijmegen 6525AJ, The Netherlands.

10.1021/nl900250g CCC: $40.75
Published on Web 04/02/2009

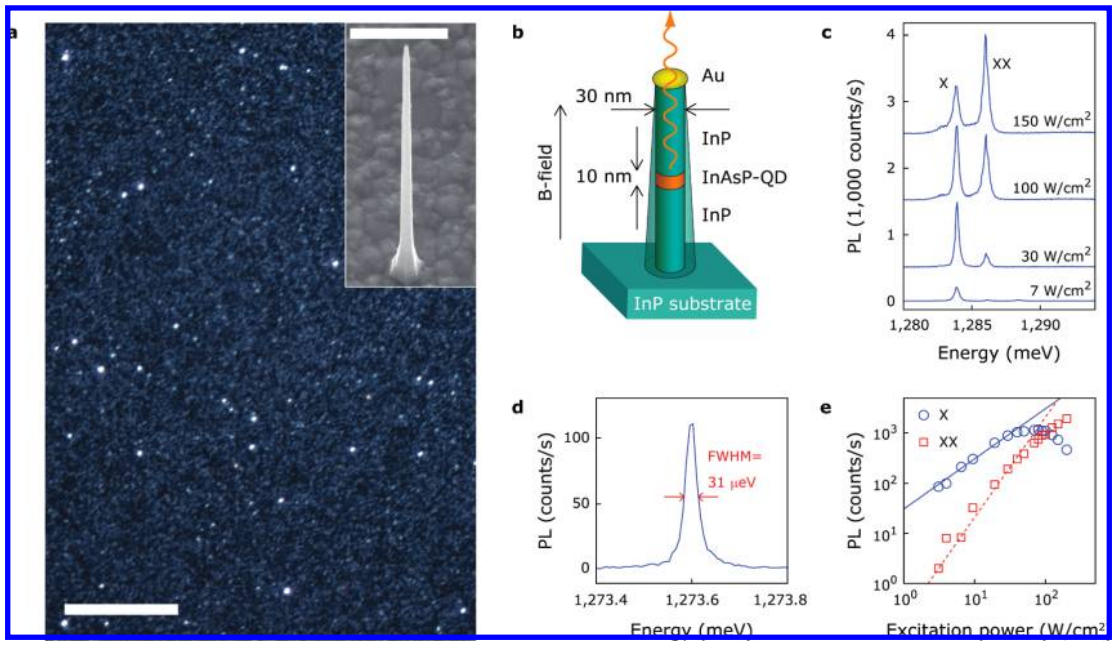

Figure 1. Structural and optical properties of nanowire quantum dots. (a) Dark-field optical microscope image of standing nanowires, observed as bright white spots (scale bar is 5 μm). Inset shows a scanning electron micrograph of a 4 μm long, standing nanowire. (b) Schematic nanowire device. Magnetic field and optical axis are parallel to the nanowire axis. (c) Photoluminescence (PL) spectra for increasing excitation power, taken at 4.2 K under nonresonance (532 nm) cw excitation. The two emission peaks correspond to the exciton (X) and biexciton (XX) transitions. (d) Example of a narrow exciton transition from a single dot. The line width is limited by our setup resolution. (e) Integrated PL intensity of X and XX versus excitation power. The solid (dashed) line is a guide to the eye for linear (quadratic) power dependence.

nanowires. The typical distance between the nanowires is larger than our spatial resolution ($\sim$0.6 μm), enabling us to select an individual dot. The dots are typically 10 nm high with a diameter of 30 nm and are surrounded by a thin shell of InP (see Figure 1b and the Supporting Information).

The presented data are all taken at 4.2 K on different quantum dots. Figure 1 shows optical spectra with peaks as narrow as 31 μeV (limited by the resolution of our spectrometer). Figure 1d shows a single peak for exciton emission (X) at low excitation power. On increasing the power the biexciton (XX) emission becomes visible with an exciton−biexciton splitting of 2.2 meV. The PL intensities of X and XX depend, as expected, linearly and quadratically on excitation power (Figure 1e), clearly identifying these optical transitions. Note also the saturation of the peak intensities at high powers, indicating that other states also become occupied.

Next, we measure the spin splitting of the exciton transition as function of a magnetic field, B, parallel to the nanowire axis (i.e., Faraday configuration). The excitation light is polarized linearly with an energy exceeding the InP bandgap. Via phonon relaxation, electrons and holes occupy the quantum states in the dot where they annihilate under emission of a photon (see panels a and b in Figure 2). We select the exciton transition from the lowest energy (s) states and measure the peak evolution as a function of B. Figure 2c shows a peak splitting linear in B on top of a quadratic B-dependence. The distance between the two peak maxima corresponds to the Zeeman spin splitting, from which we obtain an exciton g-factor, $g = (g_e + g_h) = 1.3 \pm 0.1$. A g-factor value between 1 and 2 is typical for our dots with

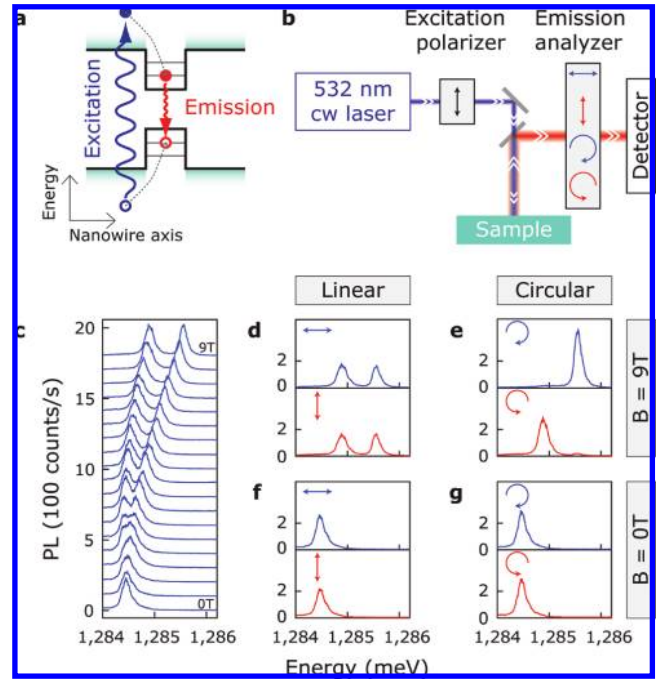

Figure 2. Polarization-sensitive magneto-photoluminescence of a single nanowire quantum dot. (a) Schematic of nonresonant excitation and recombination. (b) Experimental setup. The excitation polarization is vertically linearly polarized, whereas the polarization of the emission is analyzed. (c) PL for different magnetic fields in steps of 0.5 T. Emission polarization is not filtered. (d−g) PL with linear and circular polarization filters for 0 and 9 T.

a material fraction As/P = 1/3. Variations between dots are likely due to small variations in the material composition and different confinements.[8] The overall quadratic shift, α

$= 10\ \mu eV/T^2$, can be fitted to the diamagnetic shift of an electronic orbital with a diameter of ~20 nm.[24] This is in reasonable agreement with our quantum dot size.

The measured PL in Figure 2c is not filtered for a specific polarization. By adding such filters (see setup in Figure 2b) we analyze the polarization of the emitted photons from which we deduce the spin states of the exciton transitions. Right (σ^+) and left (σ^-) circularly polarized photons are expected, respectively, for the exciton states $\downarrow_e\uparrow_h$ and $\uparrow_e\downarrow_h$. Here, $\uparrow_e(\uparrow_h)$ represents a spin-up electron (hole) and $\downarrow_e(\downarrow_h)$ represents a spin-down electron (hole). For well-resolved spin states at 9 T, we indeed find in Figure 2e that the high-energy emission peak consists of σ^+ photons, whereas the lower energy peak is σ^- polarized. Note that the (nearly complete) absence of a second peak in Figure 2e implies full circular polarization of the two spin-resolved exciton transitions. For linear polarizers, two peaks of equal height are visible, as expected (Figure 2d). For spin-degenerate excitons at $B = 0$, the polarization analyzers make no difference for the observed PL, as shown in panels f and g in Figure 2. We emphasize that the observed absence of any linear polarization for vertical nanowires (in contrast to horizontal wires[15]) is essential for exciting and measuring specific spin states, which we discuss next.

A specific spin state can be excited when using either σ^+ or σ^- polarized light. If the emitted photons have the same polarization, it means that no spin relaxation has occurred during this excitation−relaxation cycle. Although this cycle is short (on the order of a radiative lifetime of about 1 ns) it represents a first step toward an exciton-spin memory. A complete spin memory also requires the ability to suppress the radiative decay for a controllable storage time, as has been demonstrated with self-assembled dots.[25] We have found that excitation above the InP band gap (as in Figures 1 and 2) with subsequent relaxation into the dot scrambles up the spin state and thus destroys any spin memory effect. The phase space for relaxation is largely reduced when we excite below the InP band gap into one of the confined higher energy states of the dot. Figure 3a illustrates excitation in an excited p-state with subsequent relaxation to the ground s-state. This relaxation between confined states is spin conserving, as we now demonstrate.

We characterize the higher energy states using combined PL and PLE (photoluminescence excitation) and identify a p-shell resonance around 1300 meV (see the Supporting Information). We use quasi-resonant excitation into this p-shell and measure the exciton luminescence for various polarization analyzers (see schemes a and b in Figure 3). We first reproduce Figure 2c but now for quasi-resonant excitation. Figure 3c is taken with linear excitation and analyzer such that both spin states are excited and measured. Again as a function of *B,* the exciton transition shows a Zeeman splitting and a diamagnetic shift. Note that the two split-peaks are of different height due to a slightly unequal spin excitation since the p-shell also shows spin splitting. Panels d and e in Figure 3 show the results for left and right circularly polarized excitation. When exciting with right circular polarization, only the spin up branch of the Zeeman

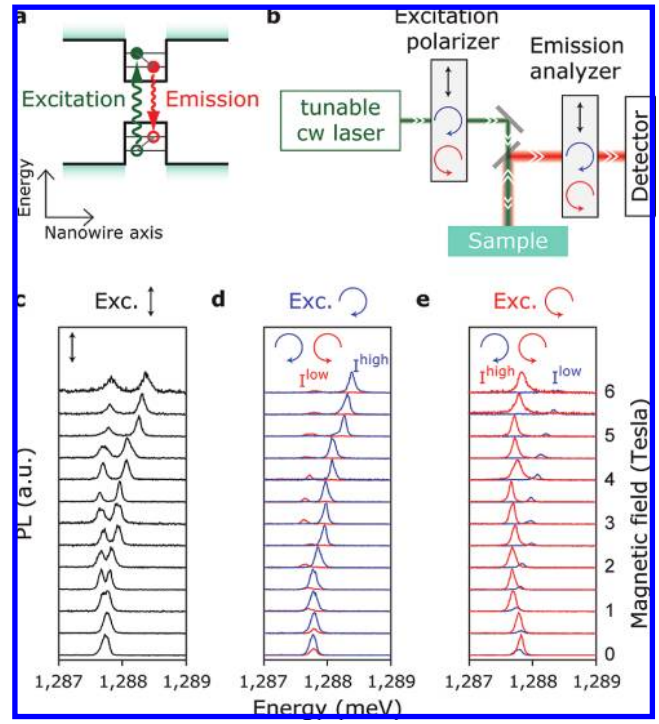

Figure 3. Polarization-selective excitation and detection of exciton spin states. (a) Schematic of quasi-resonant excitation and recombination. (b) Experimental setup. Both excitation and detection polarizations are varied. (c−e) PL for different magnetic fields. Excitation is linearly, right circularly, and left circularly polarized, respectively. Emission analyzers are set to linear (black), right (blue), or left (red) circular polarization.

split exciton is populated. In this case, we dominantly observe luminescence from the high-energy peak, which is also right-circularly polarized. We thus clearly observe spin memory. Close inspection reveals that the spin memory is not perfect and that a small peak for the wrong polarization is also observed. For nonzero B, the peak-height ratio $I^{high}/I^{low} \approx 10$. However, at $B = 0$, a reduced polarization ratio $I^{high}/I^{low} \approx 3$ was found for all seven dots that we measured. This likely indicates spin relaxation mediated by the hyperfine interaction with nuclear spins.[26] Similar measurements have been reported on ensembles of self-assembled quantum dots under quasi-resonant[27] and resonant excitation.[28] However, polarization memory was not observed at $B = 0$, possibly because of a larger exciton fine structure splitting.

As we noted, the spin memory only works for quasi-resonant excitation into the p-shell. The precise initialization of a particular spin depends on the exact excitation conditions, as exemplified by the peak height differences in Figure 3c. This excitation energy dependence can, as we discuss now, be exploited for an alternative method for spin initialization. To understand the absorption sensitivity, we show in Figure 4a quasi-resonant PLE into the p-shell for linearly polarized excitation. The excitation energy is scanned and the spin-split exciton transition is measured at 4 T. The lower left panel shows two vertical stripes that are narrow in PL energy (~0.1 meV) but broader along the vertical axis of excitation energy (~3 meV). These widths are directly related to the respective lifetimes, short in the p-shell (~ps because of fast intraband, nonradiative relaxation to the s-shell) but much

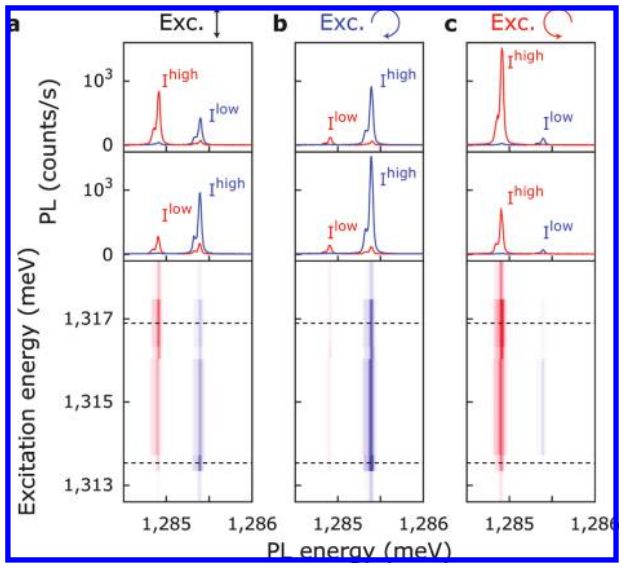

Figure 4. Energy-selective excitation and detection of exciton spin states at 4 T. Bottom panels show photoluminescence excitation (PLE) scans under (a) linearly, (b) right circularly, and (c) left circularly polarized excitation. Blue and red colors are measured separately with right and left circular polarization analyzers. Upper and middle panels show horizontal cross-sections taken, respectively, at the upper and lower dashed lines in the lower panels.

longer for the interband radiative decay. The stripes are colored red and blue, indicating the degree of measured circular polarization. Note that the red stripe is slightly shifted up in energy, indicating a higher σ^- intensity at high excitation energies. The upper panels display two cuts clearly showing a larger σ^- peak at high excitation energy and a larger σ^+ peak at low excitation energy. We find maximum polarization ratios $I^{high}/I^{low} \approx 2.5$. We emphasize that this polarization occurs despite using linear excitation light. The polarization is entirely due to selectivity in the energy of the excitation. By combining energy-selective excitation together with polarization-selective excitation, as shown in panels b and c in Figure 4, the polarization ratio is further increased to $I^{high}/I^{low} \approx 10$.

In conclusion, we have demonstrated clean quantum dots in nanowires with narrow optical transitions. Specific exciton spin states are created and measured with properly polarized light. In addition, we have demonstrated an alternative energy-selective mechanism for spin excitation. Future devices will have top and bottom electrical contacts, for instance, for the use of fast energy selectivity using the Stark effect.

Methods. ***Quantum Dot Growth.*** The nanowires were synthesized in a low-pressure (50 mbar) Aixtron 200 metal-organic vapor-phase epitaxy (MOVPE) reactor in the vapor−liquid−solid growth mode. Colloidal gold particles of 20 nm diameter were deposited on a (111)B InP substrate as catalysts for nanowire growth. The diameter of the nanowire and the quantum dot was set by the gold particle size, wherea the nanowire density was set by the gold particle density on the substrate. The dot height and nanowire length were controlled with growth time.[6] By controlling diameter, height, and As concentration, we can tune the quantum dot emission over the wide range of 900 nm to 1.5 μm.[29] Under appropriate growth conditions we were able to grow a sample with low density of nanowires containing single $InAs_{0.25}P_{0.75}$ quantum dots. These dots are designed to have luminescence around 1.2 eV. The gold particle is transparent for the light.

Experimental Setup. Micro-PL studies were performed at 4.2 K. For nonresonant excitation experiments, the nanowire quantum dots were excited with a linearly polarized 532 nm continuous wave laser focused to a spot size of 0.6 μm using a microscope objective with a numerical aperture NA = 0.85. For photoluminescence excitation experiments, a tunable titanium sapphire laser was used. The PL signal was collected by the same objective and was sent to a spectrometer, which dispersed the PL onto a nitrogen-cooled silicon array detector with 30 μeV resolution. Linear and circular emission polarizations were analyzed using a half- or quarter-waveplate, respectively, followed by a fixed polarizer. Linear and circular excitation polarization was set by placing a fixed polarizer followed by a half- or quarter-waveplate, respectively. Magnetic fields were applied in the Faraday configuration, i.e., along the quantum dot confinement axis. The data shown are all measured on different quantum dots. Similar results on polarization sensitive magneto-photoluminescence have been found on 3 dots. Polarization memory at $B = 0$ T has been measured on 7 dots, giving all similar results.

Acknowledgment. We acknowledge W. G. G. Immink for technical assistance. This work was supported by the European FP6 NODE (015783) project, the Dutch Organization for Fundamental Research on Matter (FOM), The Netherlands Organization for Scientific Research (NWO), and the Dutch ministry of economic affairs (NanoNed). The work of R.E.A. was carried out under Project MC3.0524 in the framework of the strategic research program of the Materials Innovation Institute (M2I) (www.m2i.nl). The authors declare that they have no competing financial interests.

Supporting Information Available: Additional PL spectra, EDX line scans, and TEM image (PDF). This material is available free of charge via the Internet at http://pubs.acs.org.

References

(1) Huang, M. H.; Mao, S.; Feick, H.; Yan, H.; Wu, Y.; Kind, H.; Weber, E.; Russo, R.; Yang, P. *Science* **2001**, *292*, 1897–1899.
(2) Duan, X.; Huang, Y.; Cui, Y.; Wang, J.; Lieber, C. M. *Nature (London)* **2001**, *409*, 66–69.
(3) Duan, X.; Huang, Y.; Agarwal, R.; Lieber, C. M. *Nature (London)* **2003**, *421*, 241–245.
(4) Pettersson, H.; Trägårdh, J.; Persson, A. I.; Landin, L.; Hessman, D.; Samuelson, L. *Nano Lett.* **2006**, *6*, 229–232.
(5) Borgström, M. T.; Zwiller, V.; Muller, E.; Imamoglu, A. *Nano Lett.* **2005**, *5*, 1439–1443.
(6) Minot, E. D.; Kelkensberg, F.; van Kouwen, M.; van Dam, J. A.; Kouwenhoven, L. P.; Zwiller, V.; Borgström, M. T.; Wunnicke, O.; Verheijen, M. A.; Bakkers, E. P. A. M. *Nano Lett.* **2007**, *7*, 367–371.
(7) Renard, J.; Songmuang, R.; Bougerol, C.; Daudin, B.; Gayral, B. *Nano Lett.* **2008**, *8*, 2092–2096.
(8) Björk, M. T.; Thelander, C.; Hansen, A. E.; Jensen, L. E.; Larsson, M. W.; Wallenberg, L. R.; Samuelson, L. *Nano Lett.* **2004**, *4*, 1621–1625.
(9) Michler, P.; Kiraz, A.; Becher, C.; Schoenfeld, W. V.; Petroff, P. M.; Zhang, L.; Hu, E.; Imamoglu, A. *Science* **2000**, *290*, 2282–2285.

(10) Santori, C.; Pelton, M.; Solomon, G.; Dale, Y.; Yamamoto, Y. *Phys. Rev. Lett.* **2001**, *86*, 1502–1505.
(11) Petta, J. R.; Johnson, A. C.; Taylor, J. M.; Laird, E. A.; Yacoby, A.; Lukin, M. D.; Marcus, C. M.; Hanson, M. P.; Gossard, A. C. *Science* **2005**, *309*, 2180–2184.
(12) Koppens, F. H. L.; Buizert, C.; Tielrooij, K. J.; Vink, I. T.; Nowack, K. C.; Meunier, T.; Kouwenhoven, L. P.; Vandersypen, L. M. K. *Nature (London)* **2006**, *442*, 766–771.
(13) Wang, J.; Gudiksen, M. S.; Duan, X.; Cui, Y.; Lieber, C. M. *Science* **2001**, *293*, 1455–1457.
(14) Muskens, O. L.; Treffers, J.; Forcales, M.; Borgström, M. T.; Bakkers, E. P. A. M.; Rivas, J. G. *Opt. Lett.* **2007**, *32*, 2097–2099.
(15) Van Weert, M. H. M.; Akopian, N.; Kelkensberg, F.; Perinetti, U.; van Kouwen, M. P.; Rivas, J. G.; Borgström, M. T.; Algra, R. E.; Verheijen, M. A.; Bakkers, E. P. A. M.; Kouwenhoven, L. P.; Zwiller, V. *Arxiv.* **2008**, *0808*, 2908.
(16) Bayer, M.; Stern, O.; Hawrylak, P.; Fafard, S.; Forchel, A. *Nature (London)* **2000**, *405*, 923–926.
(17) Verheijen, M. A.; Immink, G.; de Smet, T.; Borgström, M. T.; Bakkers, E. P. A. M. *J. Am. Chem. Soc.* **2006**, *128*, 1353–1359.
(18) Fasth, C.; Fuhrer, A.; Björk, M. T.; Samuelson, L. *Nano Lett.* **2005**, *5*, 1487–1490.
(19) Ng, H. T.; Han, J.; Yamada, T.; Nguyen, P.; Chen, Y. P.; Meyyappan, M. *Nano Lett.* **2004**, *4*, 1247–1252.
(20) Bryllert, T.; Wernersson, L. E.; Lowgren, T.; Samuelson, L. *Nanotechnol.* **2006**, *17*, S227−S230.
(21) Schmidt, V; Riel, H.; Senz, S.; Karg, S.; Riess, W.; Gösele, U. *Small* **2006**, *2*, 85–88.
(22) Hiruma, K.; Katsuyama, T.; Ogawa, K.; Koguchi, M.; Kakibayashi, H.; Morgan, G. P. *Appl. Phys. Lett.* **1991**, *59*, 431–433.
(23) Lauhon, L. J.; Gudiksen, M. S.; Wang, D.; Lieber, C. M. *Nature (London)* **2002**, *420*, 57–61.
(24) Walck, S. N.; Reinecke, T. L. *Phys. Rev. B* **1998**, *57*, 9088–9096.
(25) Kroutvar, M.; Ducommun, Y.; Heiss, D.; Bichler, M.; Schuh, D.; Abstreiter, G.; Finley, J. J. *Nature (London)* **2004**, *432*, 81–84.
(26) Greilich, A.; Shabaev, A.; Yakovlev, D. R.; Efros, Al. L.; Yugova, I. A.; Reuter, D.; Wieck, A. D.; Bayer, M *Science* **2007**, *317*, 1896–1899.
(27) Senès, M.; Urbaszek, B.; Marie, X.; Amand, T.; Tribollet, J.; Bernardot, F.; Testelin, C.; Chamarro, M.; Gérard, J.-M. *Phys. Rev. B* **2005**, *71*, 115334.
(28) Paillard, M.; Marie, X.; Renucci, P.; Amand, T.; Jbeli, A.; Gérard, J.-M. *Phys. Rev. Lett.* **2001**, *86*, 1634–1637.
(29) Tchernycheva, M.; Cirlin, G. E.; Patriarche, G.; Travers, L.; Zwiller, V.; Perinetti, U.; Harmand, J. C. *Nano Lett.* **2007**, *7*, 1500–1504.

NL900250G